

In-vitro bio-mineralization of arsenic and lead from aqueous solution and soil by wood rot fungus, *Trichoderma* sp.

M. Govarthanana^{a,*}, R. Mythili^b, S. Kamala-Kannan^c, T. Selvankumar^b, P. Srinivasan^b, H. Kim^{a,*}

^a Department of Environmental Engineering, University of Seoul, Seoul 02504, South Korea

^b PG & Research Department of Biotechnology, Mahendra Arts and Science College (Autonomous), Kalippatti, Namakkal 637501, Tamil Nadu, India

^c Division of Biotechnology, Advanced Institute of Environment and Bioscience, College of Environmental and Bioresource Sciences, Chonbuk National University, Iksan 54596, South Korea

ARTICLE INFO

Keywords:

Bio-mineralization
Calcite
Carbonate bound
Sequential extraction
Urease

ABSTRACT

In the present study, we investigated the role of calcite, i.e., microbially-induced precipitate by ureolytic *Trichoderma* sp. MG, in remediation of soils contaminated with arsenic (As) and lead (Pb). The fungus tolerates high concentrations of As (500 mg/L) and Pb (650 mg/L). The effects of three factors, i.e., urea concentration, CaCl₂ concentration and pH, on urease production and bio-mineralization of As and Pb were investigated using Box-Behnken design. The maximum urease production (920 U/mL) and metal removal efficiency (68% and 59% for Pb and AS, respectively) were observed in the medium containing urea of 300 mM and CaCl₂ of 75 mM at pH 9.0. Fourier transform infrared spectroscopy result revealed the formation of metal carbonates by the isolate MG. Sequential extraction of metals revealed that the carbonate fractions of As and Pb were increased to 46.4% and 42.4% in bioremediated soil, whereas in control they were 35.5% and 32.5%, respectively. The X-ray powder diffraction result further confirmed the role of calcite precipitate in bioremediation of As- and Pb-contaminated soils. The results point out that the microbially-induced calcite precipitation is a feasible, eco-friendly technology for the bioremediation of As- and Pb-contaminated sites.

1. Introduction

Arsenic (As) and lead (Pb) are well-known metals, primarily produced by mining, metal manufacturers, and human activities including modern industrial operations, and agricultural practices (Donahoe et al., 2004; Wang and Mulligan, 2006). The soil and/or water containing As and Pb pose(s) a serious threat to both the ecosystem and human health because of their high toxicity and difficulties in treatment (Hseu et al., 2010). The toxicity of the metals is associated with many kinds of human diseases including malfunctions of liver, heart, central nervous system, and kidney, skin and lung tumours, and cardiovascular disease (Dopp et al., 2004, 2010). Hence, a technology to efficiently remove As and Pb from contaminated soil and water has attracted increased attention worldwide.

The physico-chemical practices commonly applied for removal of As and Pb are ion exchange, chemical precipitation, electrochemical treatment, and reverse osmosis (Zhang et al., 2017). However, the applicability of these methods is limited because of their high cost, time demand and potential generation of secondary wastes (Cui et al., 2017). Recently, biological remediation of As and Pb is considered as a

promising alternative due to its environmental friendliness and cost effectiveness (Govarthanana et al., 2010; Selvankumar et al., 2017). It has been well established that microorganisms can remediate As and Pb in soils through different routes such as intra and/or extra-cellular accumulation (Brookshaw et al., 2012), biosorption (Azarpira and Mahdavi, 2016; Balarak et al., 2016; Bazrafshan et al., 2017), bio-mineralization (Govarthanana et al., 2010), and chelation by producing organic acids (Gadd et al., 2012). However, the effectiveness of bioremediation of As and Pb varies depending on microbial sensitivity to soil redox potentials and/or valence state of metals (Qian et al., 2017).

Microbiologically-induced calcite precipitation (MICP) is a widely known in-situ bioremediation method, where metal-resistant microbes immobilize toxic metals in the form of minerals (Zhu and Ditttrich, 2016). Recent progress in the science of MICP in bio-geological formations has shaped the interest of bioremediation researchers worldwide (Dhami et al., 2017). The precipitation of target metal compounds with calcium carbonate and its dominant derivatives (i.e., calcites) is mediated by a variety of bacteria, fungi, algae, and protista, thus, this mechanism is preferably defined as bio-mineralization and/or MICP (Gadd, 2010; Qian et al., 2015). Among the microorganisms, fungi have

* Corresponding authors.

E-mail addresses: gova.muthu@gmail.com (M. Govarthanana), h_kim@uos.ac.kr (H. Kim).

<https://doi.org/10.1016/j.ecoenv.2019.03.034>

Received 25 September 2018; Received in revised form 6 March 2019; Accepted 7 March 2019

Available online 14 March 2019

0147-6513/ © 2019 Elsevier Inc. All rights reserved.

higher biomass and resistance to metals compared to bacteria and algae; thus, fungi could be the potential candidate for MICP in the treatment of As- and Pb-contaminated soils (Kumari et al., 2015).

Recent studies have reported the *Trichoderma* sp. could survive under As-stress conditions in the mode of biotransformation and speciation (Su et al., 2010, 2017). Most of the studies reported that *Trichoderma* sp. can remediate single metal by MICP (Su et al., 2015). Resistance to more than one metal would be advantageous in clean-up of multi-metal-contaminated soils. To the best of our knowledge, no study has been performed in the past on bioremediation of As- and Pb-contaminated soils based on calcite precipitation mediated by *Trichoderma* sp. Recently, we successfully isolated As- and Pb-resistant *Trichoderma* sp. MG from decayed wood. Hence, the present study deals (i) screening of the isolate, *Trichoderma* sp. MG, for ureolytic activity, (ii) assessing the potential of the isolate MG to immobilize As and Pb via MICP under optimized physico-chemical conditions using the Box-Behnken design (BBD), (iii) evaluating different fractions of As and Pb in bioremediated soils to better understand the interaction between the isolate MG and metals, and (iv) confirming the MICP process by applying Fourier transform infrared spectroscopy (FT-IR) and X-ray diffraction (XRD) characterization for the bioremediated soils.

2. Materials and methods

2.1. Fungal strain

The isolation and identification of the isolate MG, and minimal inhibitory concentration of As and Pb for the fungal strain were reported in our previous study (Govarathanan et al., 2018).

2.2. Screening of ureolytic activity of isolate MG

The isolate MG was screened for urease activity using the Christensen's urea agar medium (Christensen, 1946). Briefly, well grown fungal discs (10 mm diameter) were transferred to the Christensen's urea agar and the plates were incubated at $26 \pm 2^\circ\text{C}$ for 8–16 d. After incubation, the color change in the medium indicates the ureolytic activity of the isolate.

2.3. Optimization of urease activity and enhanced removal of As and Pb using Response surface methodology (RSM)

The BBD-based response surface methodology (RSM) was used to optimize the pH, urea, and CaCl_2 concentrations for enhanced production of urease and removal of As and Pb from soils. In brief, batch experiments were performed in 250 mL bottles containing 100 mL of mineral-precipitating media (MPM1) (Dhami et al., 2017) with different concentrations of urea (100–500 mM), CaCl_2 (50–100 mM), and pH (6–9). Metal solutions (100 mg/L) were carefully injected into the bottles after sterilization. Later, five discs of the isolate MG was aseptically inoculated into each bottle and incubated in a rotary shaker at 27°C for 14 d. A total of 17 runs were executed to determine the optimal process factors; tests for As and Pb removal and urease activity were carried out according to the actual experimental design matrix. The result was analyzed by applying ANOVA and response plots. For RSM, the most widely used second-order polynomial equation was developed to fit the experimental result and identify the relevant model parameters.

$$Y = \beta_0 + \sum \beta_j X_j + \sum \beta_{ij} X_i^2 + \sum \beta_{ij} X_i X_j \quad (1)$$

where Y is the predicted response; β_0 , β_i , and β_{ij} are the coefficients of the regression model; and X_i and X_j represent independent variables.

The urease activity of the *Trichoderma* sp. was determined by measuring the amount of ammonia released from urea during the phenol-hypochlorite assay (Natarajan, 1995). One unit of urease

activity was defined as the amount of enzyme liberating $1 \mu\text{mol NH}_3$ from urea per minute. As and Pb concentrations in the samples were analyzed using inductive coupled plasma-mass spectroscopy (ICP-MS).

2.4. Characterization of fungal biomass using FT-IR

At the end of bioremediation experiments, the *Trichoderma* biomass was collected, washed several times with sterile distilled water, and dried for 24–48 h in a freeze dryer. The dried fungal biomass was analyzed by using FT-IR, and the spectrum was obtained using the KBr method on a Perkin-Elmer FT-IR spectrophotometer (Norwalk, VA, USA) in the region of $4000\text{--}400 \text{ cm}^{-1}$.

2.5. Bio-mineralization of As- and Pb-contaminated soil by *Trichoderma* sp

Soil samples were collected from a depth of 20 cm, air-dried, sieved to $< 2 \text{ mm}$, sterilized at 120°C for 70 min (four consecutive days), and dried in an oven at 40°C for a week. Two different groups of experiments were performed for the bioremediation studies: bio-mineralization and control experiments. Bio-mineralization experiments were performed with the following matrix: 10 g of soil in 100 mg kg^{-1} of As or Pb in MPM1 + 10 discs of *Trichoderma* culture + 300 mM urea and 75 mM CaCl_2 solution. On the other hand, control experiments were performed with the following matrix: 10 g of soil in 100 mg kg^{-1} of As or Pb in MPM1. The flasks were incubated in a rotary shaker (180 rpm) at room temperature for 14 d. After incubation, the samples were dried at 60°C for 48 h and used for metal sequential extraction studies. The exchangeable (F1), carbonate (F2), iron and manganese oxide-bound (F3), organic-bound (F4), and residual fractions (F5) of As and Pb in the soil samples were determined according to Song et al. (2009).

2.6. X-ray diffraction investigation of soil

The soil samples were analyzed by XRD to identify the metal crystals produced by *Trichoderma* sp. The XRD analysis was carried out according to Govarathanan et al. (2010).

2.7. Statistical analysis

The optimization experiments were performed using a statistical software Design Expert (Version 6.0, Stat-Ease Inc., Minneapolis, USA). The effective variables for the enhanced bio-mineralization were studied with response surface methodology (RSM) Box-Behnken design (BBD). By using the optimal BBD, the points of the bio-mineralization experiments that will reduce the error in the estimated co-efficient of the response model will be selected. An ANOVA test for urease production, As and Pb removal were performed to ensure a good model.

3. Results and discussion

3.1. Screening of ureolytic activity of isolate MG

The formation of pink color around the mycelia plug in Christensen's urea agar medium plate indicates the ureolytic activity of the isolate MG. The urea agar base was supplemented with sterile urea. Phenol red was added in the urea agar medium as a pH indicator. The urea hydrolysis will increase the pH of the medium to render it alkaline, resulting in development of pink color. The alkaline pH indicates the production of ammonia (Christensen, 1946; Li et al., 2015).

3.2. Response surface optimization of urease production, As and Pb removal

The effect of bioremediation factors such as concentrations of urea and CaCl_2 , and pH on urease production and removal of As and Pb was investigated using the BBD (Fig. 1). Based on the experimental design, the maximum urease production (920 U/mL) and high metal removal

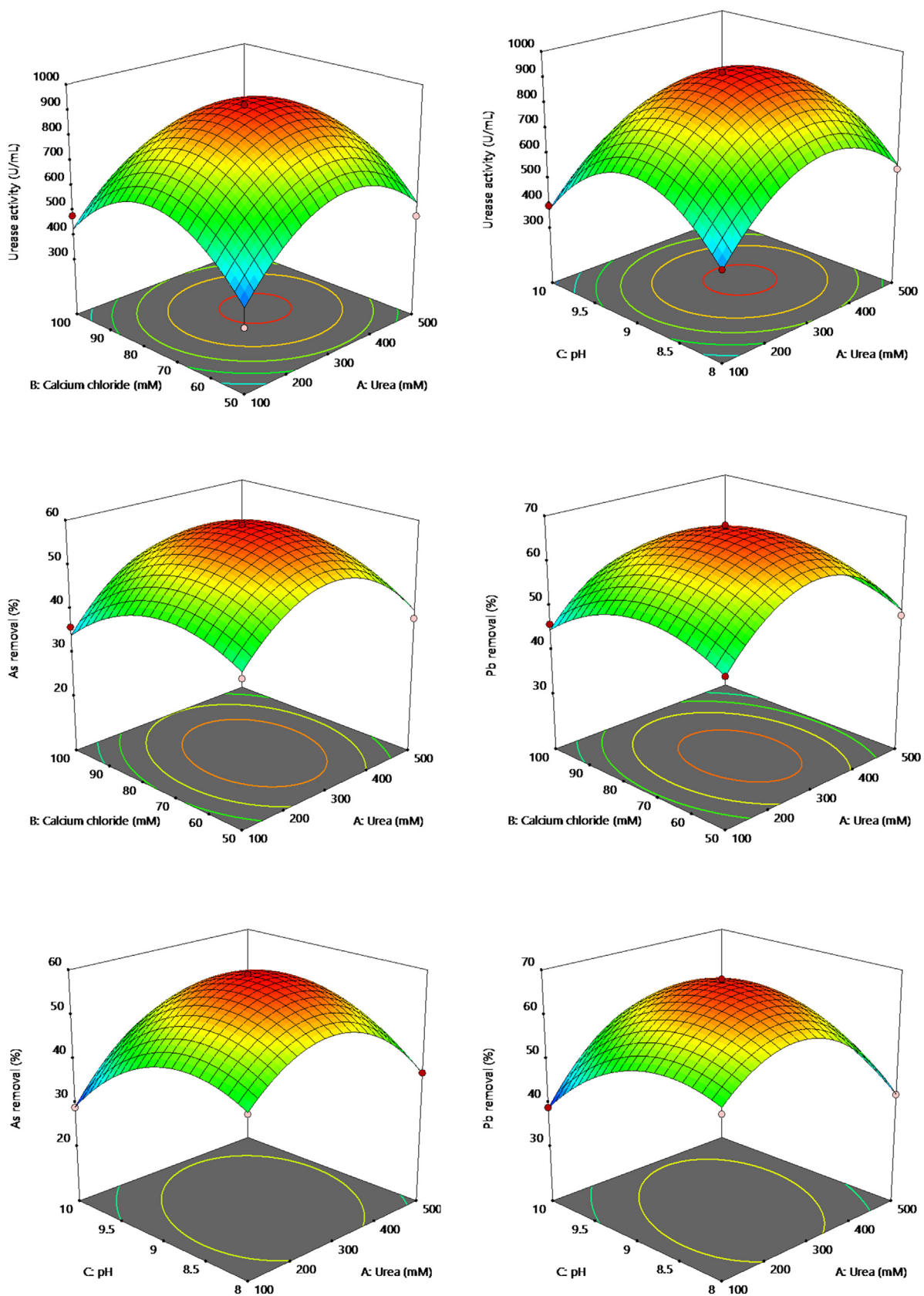


Fig. 1. Response surface 3-D plots of urease production, As and Pb removal by the isolate *Trichoderma* sp. MG.

efficiencies (68% for Pb and 59% for As) were observed at the experimental condition of 300 mM of urea and 75 mM of CaCl₂ at pH 9.0. However, much lower urease production (390 U/mL) and metal-

removal efficiencies (39.0% for Pb and 29% for As) were achieved at 100 mM of urea and 75 mM of CaCl₂ at pH 10. The result showed that the metal removal was directly proportional to the amount of urease

produced. The maximum metal removal efficiency of ~60% was observed along with high urease production, while the minimum efficiency of 30% was along with low urease production. The MICP process had a positive effect on the removal of As and Pb by urease production. The different removal efficiencies by the isolate *Trichoderma* sp. MG for Pb (68.0%) and As (59%) might be due to different physiological adaptation mechanisms and metal tolerance mechanisms. Several studies have reported the varying toxicity tolerance of fungal isolates to different metals (Gonzalez-Chavez et al., 2002; Balamurugan and Schaffner, 2006). The MICP process depends on the microorganisms modifying their local environment to create an appropriate physico-chemical condition for the precipitation of metals (Gadd et al., 2010, 2012). Li et al. (2014) demonstrated that the urease-positive fungus, *Neurospora crassa* has the ability to precipitate metal carbonates when it is incubated in urea-amended media, suggesting that metal remediation or recovery by fungi is a promising method.

Li et al. (2015) reported that the media amended with urea and CaCl_2 involve precipitation of metals by the fungus, *M. gramineum*. Several studies have reported the concentration of available calcium sources significantly affect the microbial growth and carbonate precipitation (Gorospa et al., 2013; Li et al., 2013). It was reported that CaCl_2 could induce the growth of *Aspergillus* sp. UF3 and calcite precipitation under Pb stress (Dhami et al., 2017). Regarding the pH, a rather high pH is preferable; Achal et al. (2012) reported that the best pH would be 9.2 for the bio-mediated precipitation of most heavy metals. In short, the literature and the result from this study demonstrate that the optimization of physico-chemical conditions for the metal remediation or recovery by fungi would be a promising method.

3.3. ANOVA test for urease production and enhanced As and Pb removal

The BBD experimental design and results of urease production and As and Pb removal obtained from each run are presented in Table 1. The results were analyzed and the responses were generated. An ANOVA test for urease production and As and Pb removal designs was performed to ensure a good model. The test result for the quadratic regression model (Eq. (1)) exhibits that it is highly significant, as evident from the Fisher's F-test ($p < 0.005$). There was only a 0.01% chance that a model F-value could occur due to noise. The lack of fit values of urease production 146.04, As removal 36.25, and Pb removal 17.92 implies that lack of fit is also significant. There are only a 0.02%, 0.23%, and 0.88% chance that lack of fit F-value could occur due to noise respectively. The predicted R^2 and adjusted R^2 values were in reasonable agreement with the value of R^2 , which is closer to 1.0, indicating the better fitness of the model in the experimental data. In

Table 1

Box-Behnken design and response result values of urease production, As and Pb removal.

Run	Urea (mM)	CaCl_2 (mM)	pH	Urease (U/mL)	As (%)	Pb (%)
1	500	100.0	9.0	620.0	42.0	44.0
2	500	75.0	8.0	540.0	37.0	42.0
3	300	75.0	9.0	920.0	59.0	67.0
4	300	50.0	8.0	520.0	45.0	55.0
5	100	100.0	9.0	480.0	36.0	46.0
6	300	75.0	9.0	900.0	58.0	67.0
7	500	50.0	9.0	480.0	38.0	48.0
8	100	75.0	10.0	390.0	29.0	39.0
9	300	75.0	9.0	920.0	59.0	68.0
10	500	75.0	10.0	490.0	41.0	51.0
11	100	50.0	9.0	320.0	39.0	49.0
12	300	100.0	10.0	340.0	34.0	44.0
13	100	75.0	8.0	420.0	42.0	52.0
14	300	100.0	8.0	440.0	44.0	54.0
15	300	75.0	9.0	920.0	59.0	67.0
16	300	75.0	9.0	920.0	59.0	67.0
17	300	50.0	10.0	480.0	45.0	55.0

Table 2

ANOVA for response surface quadratic model of urease production, As and Pb removal.

Source of variation	Sum of squares	Degrees of freedom	Mean squares	F value	p-value
Model	7.774E+ 05	9	86382.42	17.10	0.0006 ^a
A	33800.00	1	33800.00	335.11	< 0.0001
B	800.00	1	800.00	309.08	< 0.0001
C	6050.00	1	6050.00	312.97	< 0.0001
AB	100.00	1	100.00	88.13	< 0.0001
AC	100.00	1	100.00	87.71	< 0.0001
BC	900.00	1	900.00	3.34	0.1102
A ²	1.910E+ 05	1	1.910E+ 05	16.79	0.0046
B ²	2.189E+ 05	1	2.189E+ 05	29.42	0.0010
C ²	2.486E+ 05	1	2.486E+ 05	28.20	0.0011
Residual	35370.00	7	5052.86	—	—
Lack of fit	35050.00	3	11683.33	531.93	< 0.0001
Pure error	320.00	4	80	—	—
Core total	8.128E + 05	16	—	—	—

addition, sequential model sum of squares, lack of fit tests and model summary statistics further supported the significance and adequacy of the model (Table 2). Three dimensional plots provided in Fig. 1 graphically represent the regression equations and were used to visualize the relationship between the response and experimental levels of each variable and the type of interaction between the variables to determine the optimum urease production and As and Pb removal efficiencies. The coefficients of all the regression equations were determined to obtain the followings.

$$\text{Urease activity (U mL}^{-1}\text{)} = 916.00 + 65.00 \text{ A} + 10.00 \text{ B} - 27.50 \text{ C} - 5.00 \text{ AB} - 5.00 \text{ AC} - 5.00 \text{ BC} - 213.00 \text{ A}^2 - 228.00 \text{ B}^2 - 243 \text{ C}^2 \quad (2)$$

$$\text{As removal efficiency (\%)} = 58.80 + 1.50 \text{ A} - 1.37 \text{ B} - 2.38 \text{ C} + 1.75 \text{ AB} + 4.25 \text{ AC} - 2.50 \text{ BC} - 12.40 \text{ A}^2 - 7.65 \text{ B}^2 - 9.15 \text{ C}^2 \quad (3)$$

$$\text{Pb removal efficiency (\%)} = 67.20 - 0.1250 \text{ A} - 2.37 \text{ B} - 1.75 \text{ C} - 0.2500 \text{ AB} + 5.50 \text{ AC} - 2.50 \text{ BC} - 13.23 \text{ A}^2 - 7.22 \text{ B}^2 - 7.97 \text{ C}^2 \quad (4)$$

where A, B and C are the coded terms used in this experiment and represent urea (mM) and CaCl_2 concentration (mM) and pH (unit), respectively. The effect of process variables on the response factors are shown in 3D plots. The normality assumption of the response model was checked by obtaining a normal probability plot of the residuals. Equality of variance was checked by plotting residuals against the treatments and the treatment averages, (fitted values), and inspecting the spread in the residuals (Supplementary Fig. 1–3). The results indicated that the developed statistical model is appropriate and the assumptions associated with the ANOVA model are not violated.

3.4. FT-IR analysis

The As and Pb removal mechanism of *Trichoderma* sp. MG in MPM1 was analyzed using FT-IR. Fig. 2 showed the absorption pattern of As group. The sharp peaks at 1554, 1394 cm^{-1} could be the C–O stretching of the COOH groups. The absorption peaks at 1074 and 762 cm^{-1} are attributed to hydroxyl ethers, amines, and amides, respectively (Li et al., 2015). Fig. 3 shows the absorption pattern of Pb treatment group. The bands observed at 3475 and 2934 cm^{-1} were assigned to the C–H, O–H, and N–H stretching vibrations of COOH groups. The sharp absorption peaks at 1753 and 991 cm^{-1} could be due to the N–H stretching of primary secondary amines and amides (Qian et al., 2017; Li et al., 2015). The FT-IR results revealed that the carboxyl, alkanes, and amide groups served as the preliminary molecules for the

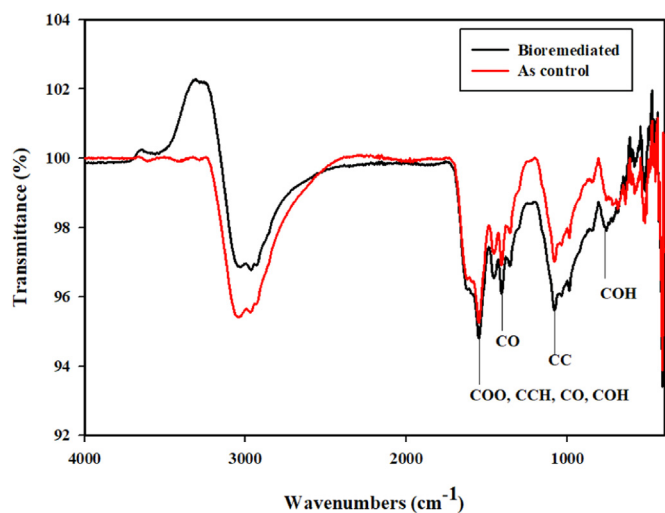


Fig. 2. FT-IR spectrum of *Trichoderma* sp. MG grown in As-containing media with and without urea and CaCl_2 .

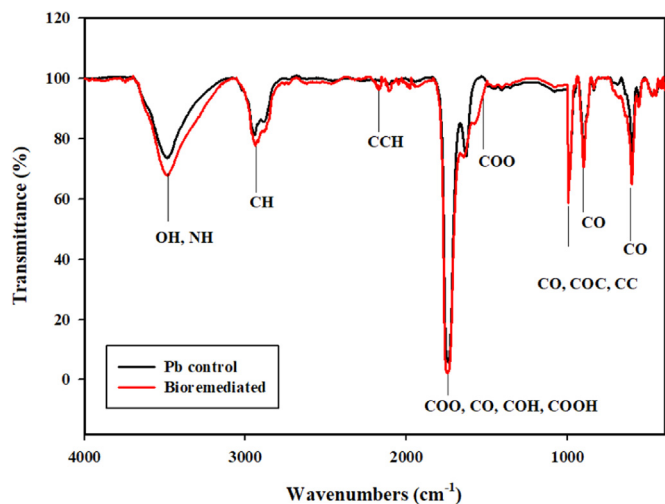


Fig. 3. FT-IR spectrum of *Trichoderma* sp. MG grown in Pb-containing media with and without urea and CaCl_2 .

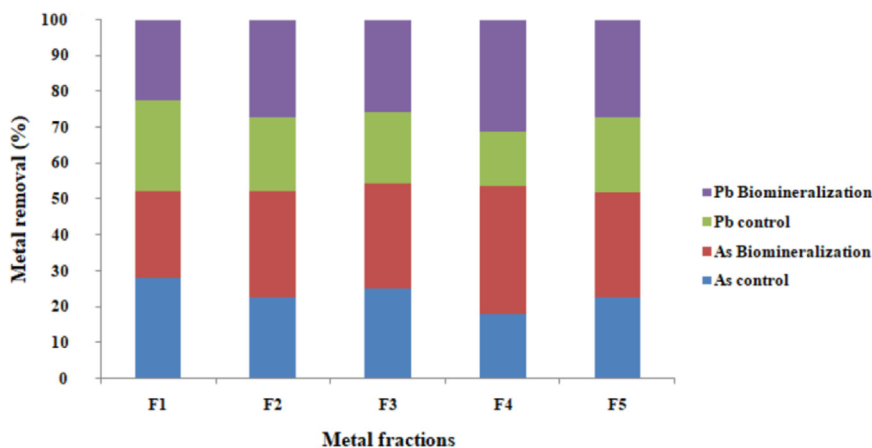


Fig. 4. Distribution of As and Pb fractions in control and bio-mineralized soils (F1- exchangeable fraction, F2- carbonate fraction, F3- iron and manganese oxide-bound fraction, F4- organic-bound fraction, and F5-residual fraction).

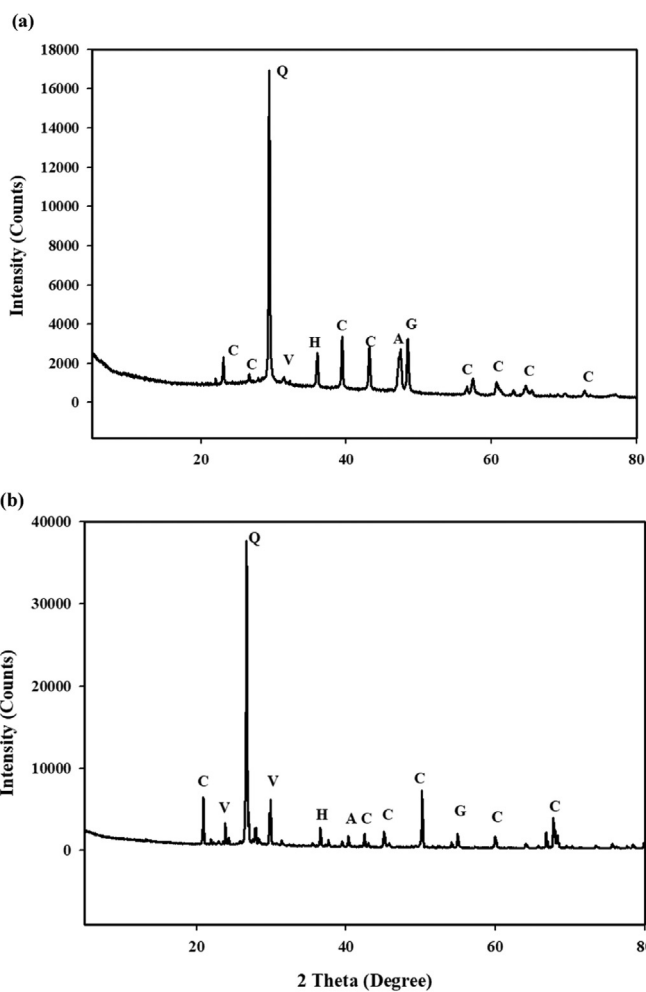


Fig. 5. X-ray diffractogram of bio-mineralized soils (a) As contaminated soil, (b) Pb contaminated soils (C-calcite, H-halite, Q-quartz, V-vaterite, A-aragonite).

subsequent precipitation of As and Pb.

3.5. Sequential extraction

A methodology to sequentially extract As and Pb was adopted to provide a comprehensive knowledge of the availability of As and Pb

and their interaction with carbonates biologically formed in contaminated soils. The order of As and Pb distribution were $F2 > F1 > F4 > F3 > F5$. F1 for As and Pb (As bio-mineralization group: 27.6% and Pb bio-mineralization group: 25.6%) was lower than the respective control group (As control: 32.5% and Pb control: 29.5%). This result indicates that the isolate *Trichoderma* sp. MG could transform the bio-available metals into non-bio-available forms. The significantly decreased F1 value indicates that the bioaccumulation and biomagnifications of metals are prevented in the metal-contaminated soils. The results are consistent with previous studies reporting a significant reduction in exchangeable fraction of metals after bioaugmentation (Achal et al., 2012; Qian et al., 2017). However, a considerable increase in the carbonate fraction (F2) was observed in the As (46.4%) and Pb (42.4%) bioremediated soils, whereas for the control soils, it was 35.5% and 32.5%, respectively (Fig. 4). The increased distribution of carbonate-bound As and Pb was due to the induced carbonate precipitation. The results corroborate with the studies by Qian et al. (2017) and Govarathanan et al. (2013), reporting a significant increase in the carbonate fraction of metals (F2) after bioaugmentation.

The distribution of Fe-Mn oxide fraction was not altered significantly in control (As: 14.5, Pb: 11.5%) and bioremediated soils (As: 16.8% and Pb 14.8%). It might be due to the unavailability of Fe-Mn fractions (F3) of As and Pb to the isolate MG. The results are consistent with a previous study reporting that bioaugmentation did not significantly reduce the Fe-Mn oxide fraction of metals (Qian et al., 2017). F4 of As and Pb were significantly altered in the bioremediated soil (As 24.4% and Pb 21.4%). The increased F4 values could be due to bioadsorption to the fungal mycelia biomass. The increased residual fraction (F5) was observed in bioremediated (As: 28.9, Pb: 26.9%) soils compared to the control soils (As: 22.6, 20.6%) respectively. The observed results indicated the efficiency of *Trichoderma* Sp. MG on bio-mineralization of As and Pb in contaminated soil.

3.6. XRD of soil

The result from sequential metal extractions might not be sufficient enough to confirm the role of carbonate precipitation and mineral formation. Thus, detailed XRD patterns of the bioremediated soils were investigated and the results are shown in Fig. 5. Accordingly, the XRD results showed the formation of various minerals such as, calcite, aragonite, halite, and quartz. Many calcite peaks could be observed in the bioremediated soils (Fig. 5(a), (b)). Alexandratos et al. (2007) reported that oxy-anions of the metals may substitute for the carbonate group in the calcite structure formation. It has been suggested that the calcite peaks could be due to the indirect action of urease. Qian et al. (2017) reported that the formation of calcite peaks during bio-mineralization induced by fungal degradation of urea.

4. Conclusion

In this study, the mechanism of As and Pb bio-mineralization by the isolate, *Trichoderma* sp. MG and the optimal physico-chemical conditions were determined in both aqueous solution and soil. The isolate, *Trichoderma* sp. MG could effectively immobilize As and Pb in the contaminated soils. The fungal-mediated carbonates and minerals were identified by FT-IR analysis and XRD. The MICP-associated removal of As and Pb by *Trichoderma* sp. MG presented in this paper is an eco-friendly and cost-effective bioremediation technique to clean up the soil contaminated by the heavy metals.

Acknowledgments

This research was financially supported by Korea Ministry of Environment (Project No: 2015001790002), which is greatly appreciated. This paper was also supported by research funds of Chonbuk National University in 2017.

Appendix A. Supporting information

Supplementary data associated with this article can be found in the online version at doi:10.1016/j.ecoenv.2019.03.034.

References

- Achal, V., Pan, X., Zhang, D., Fu, Q.L., 2012. Biomineralization based remediation of As (III) contaminated soil by *Sporosarcina ginsengisoli*. *J. Hazard. Mater.* 201–202, 178–184.
- Alexandratos, V.G., Elzinga, E.J., Reeder, R.J., 2007. Arsenate uptake by calcite: macroscopic and spectroscopic characterization of adsorption and incorporation mechanisms. *Geochim. Cosmochim. Acta* 71, 4172–4187.
- Azarpira, H., Mahdavi, Y., 2016. Removal of Cd(II) by adsorption on agricultural waste biomass. *Pharma Chem.* 8 (12), 61–67.
- Balamurugan, K., Schaffner, W., 2006. Copper homeostasis in eukaryotes: teetering on a tightrope. *Biochim. Biophys. Acta (BBA) – Mol. Cell Res.* 1763, 737–746.
- Balarak, D., Joghataei, A., Azarpira, H., Mostafapour, F.K., 2016. Isotherms and thermodynamics of Cd (II) ion removal by adsorption onto *Azolla filiculoides*. *Int. J. Pharm. Technol.* 8 (3), 15780–15788.
- Bazrafshan, E., Sobhanikia, M., Mostafapour, F.K., Kamani, H., 2017. Chromium bio-sorption from aqueous environments by mucilaginous seeds of *Cydonia oblonga*: kinetic and thermodynamic studies. *Glob. Nest J.* 19 (2), 269–277.
- Brookshaw, D.R., Patrick, R.A.D., Lloyd, J.R., Vaughan, D.J., 2012. Microbial effects on mineral–radionuclide interactions and radionuclide solid-phase capture processes. *Mineral. Mag.* 76, 777–806.
- Christensen, W.B., 1946. Urea decomposition as a means of differentiating *Proteus* and *Paracolon* cultures from each other and from *Salmonella* and *Shigella* types. *J. Bacteriol.* 52, 461–466.
- Cui, Z., Zhang, X., Yang, H., Sun, L., 2017. Bioremediation of heavy metal pollution utilizing composite microbial agent of *Mucorcircinelloides*, *Actinomucor* sp. and *Mortierella* sp. *J. Environ. Chem. Eng.* 5, 3616–3621.
- Dhami, N.K., Christelle Quirin, M.E., Mukherjee, A., 2017. Carbonate biomineralization and heavy metal remediation by calcifying fungi isolated from karstic caves. *Ecol. Eng.* 103, 106–117.
- Donahoe, J., D'Imperio, S., Jackson, C., Inskeep, W., McDermott, T., 2004. Arsenite-oxidizing *Hydro genobaculum* strain isolated from an acid–sulfate–chloride geothermal spring in Yellow stone National Park. *Appl. Environ. Microbiol.* 70, 1865–1868.
- Dopp, E., Hartmann, L.M., Florea, A.M., Von Recklinghausen, U., Piper, R., Shokouhi, B., Rettenmeier, A.W., Hirner, A.V., Obe, G., 2004. Uptake of inorganic and organic derivatives of arsenic associated with induced cytotoxic and genotoxic effects in Chinese hamster ovary (CHO) cells. *Toxicol. Appl. Pharmacol.* 201, 156–165.
- Dopp, E., Kligerman, A.D., Diaz-Bone, R., 2010. Organo arsenicals, Uptake metabolism, and toxicity. *Met. Ions Life Sci.* 7, 231–265.
- Gadd, G.M., 2010. Metals, minerals and microbes: geomicrobiology and bioremediation. *Microbiology* 156, 609–643.
- Gadd, G.M., Rhee, Y.J., Stephenson, K., Wei, Z., 2012. Geomycology: metals, actinides and biominerals. *Environ. Microbiol. Rep.* 4, 270–296.
- Gonzalez-Chavez, C., D'Haen, J., Vangronsveld, J., Dodd, J.C., 2002. Copper sorption and accumulation by the extra radical mycelium of different *Glomus* spp. (arbuscular mycorrhizal fungi) isolated from the same polluted soil. *Plant Soil* 240, 287–297.
- Gorospe, C.M., Han, S.H., Kim, S.G., et al., 2013. Effects of different calcium salts on calcium carbonate crystal formation by *Sporosarcina pasteurii* KCTC 3558. *Biotechnol. Bioprocess Eng.* 18, 903–908.
- Govarathanan, M., Lee, K.J., Cho, M., Kim, J.S., Kamala-Kannan, S., Oh, B.T., 2013. Significance of autochthonous *Bacillus* sp. KK1 on biomineralization of lead in mine tailings. *Chemosphere* 90, 2267–2272.
- Govarathanan, M., Mythili, R., Selvakumar, T., Kamala-Kannan, S., Kim, H., 2018. Myco-phytoremediation of arsenic- and lead- contaminated soils by *Helianthus annuus* and wood rot fungi, *Trichoderma* sp. isolated from decayed wood. *Ecotoxicol. Environ. Saf.* 151, 279–284.
- Govarathanan, M., Park, S.H., Park, Y.J., et al., 2010. Lead biotransformation potential of allochthonous *Bacillus* sp. SKK11 with sesame oil cake extract in mine soil. *RSC Adv.* 5, 54564–54570.
- Hseu, Z.Y., Shaw-Wei, S.U., Lai, H.Y., Guo, H.Y., Chen, T.C., Chen, Z.S., 2010. Remediation techniques and heavy metal uptake by different rice varieties in metal-contaminated soils of Taiwan: new aspects for food safety regulation and sustainable agriculture. *Soil. Sci. Plant Nutr.* 56, 31–52.
- Kumari, D., Pan, X., Achal, V., et al., 2015. Multiple metal-resistant bacteria and fungi from acidic copper mine tailings of Xinjiang. *China Environ. Earth Sci.* 74, 3113–3121.
- Li, Q., Csetenyi, L., Gadd, G.M., 2014. Biomineralization of metal carbonates by *Neurospora crassa*. *Environ. Sci. Technol.* 48, 14409–14416.
- Li, Q., Csetenyi, L., Paton, G.I., Gadd, G.M., 2015. CaCO₃ and SrCO₃ bioprecipitation by fungi isolated from calcareous soil. *Environ. Microbiol.* 17, 3082–3097.
- Li, W., Chen, W.S., Zhou, P.P., Cao, L., Yu, L.J., 2013. Influence of initial pH on the precipitation and crystal morphology of calcium carbonate induced by microbial carbonic anhydrase. *Colloids Surf. B* 102, 281–287.
- Natarajan, K.R., 1995. Kinetic study of the enzyme urease from *Dolichos biflorus*. *J. Chem. Educ.* 72, 556–557.
- Qian, X., Fang, C., Huang, M., Achal, V., 2017. Characterization of fungal-mediated carbonate precipitation in the biomineralization of chromate and lead from an aqueous solution and soil. *J. Clean. Prod.* 164, 198–208.
- Qian, X.Y., Zhang, Q., Wilkinson, S., Achal, V., 2015. Cleaning of historic monuments:

- looking beyond the conventional approach? J. Clean. Prod. 101, 180–181.
- Selvankumar, T., Radhika, R., Mythili, R., Arunprakash, S., Srinivasan, P., Govarathan, M., Kim, H., 2017. Isolation identification and characterization of arsenic transforming exogenous endophytic *Citrobacter* sp. RPT from roots of *Pteris vittata*. 3 Biotech 7, 264.
- Song, Y.C., Sivakumar, S., Nguyen, T.T., Kim, S.H., Kim, B.G., 2009. The immobilization of heavy metals in biosolids using phosphate amendments – comparison of EPA (6010 and 3051) and selective sequential extraction methods. J. Hazard. Mater. 167, 1033–1037.
- Su, S., Zeng, X., Bai, L., Williams, P.N., Wang, Y., Zhang, L., Wu, C., 2017. Inoculating chlamydo spores of *Trichoderma asperellum* SM-12F1 changes arsenic availability and enzyme activity in soils and improves water spinach growth. Chemosphere 175, 497–504.
- Su, S., Zeng, X., Feng, Q., et al., 2015. Demethylation of arsenic limits its volatilization in fungi. Environ. Pollut. 204, 141–144.
- Su, S.M., Zeng, X.B., Bai, I.Y., Jiang, X.L., Li, L.F., 2010. Bioaccumulation and biovolatilization of pentavalent arsenic by *Penicillium janthinellum*, *Fusarium oxysporum*, and *Trichoderma asperellum* under laboratory conditions. Curr. Microbiol. 61, 261–266.
- Wang, S., Mulligan, C.N., 2006. Occurrence of arsenic contamination in Canada: sources, behaviour and distribution. Sci. Total Environ. 366, 701–721.
- Zhang, H., Ma, D., Qiu, R., Tang, Y., Du, C., 2017. Non-thermal plasma technology for organic contaminated soil remediation: a review. Chem. Eng. J. 313, 157–170.
- Zhu, T., Dittrich, M., 2016. Carbonate precipitation through microbial activities in natural environment, and their potential in biotechnology: a review. Front. Bioeng. Biotechnol. 4, 4.